LINK QUALITY METRICS FOR ADAPTIVE CODING AND MODULATION WITH SOQPSK AND OFDM

Enkuang D Wang, Timothy J Brothers, and Richard T Causey
Georgia Tech Research Institute
Atlanta, Georgia 30318
{enkuang.wang, timothy.brothers, richard.causey}@gtri.gatech.edu

ABSTRACT

In previous work, we presented a link quality metric for adaptive modulation and coding of two standard telemetry waveforms, orthogonal frequency-division multiplexing (OFDM) and shaped-offset quadrature phase shift keying (SOQPSK). That metric unified error vector magnitude (EVM) and Godard dispersion, for OFDM and SOQPSK, respectively, in the contexts of additive white Gaussian noise (AWGN) channels. In this paper, we present an alternative metric based on low density parity check (LDPC) decoding iterations. We show this new metric to be an equally effective substitute for AWGN channels but also to be applicable to a wider variety of channels, including those with multipath and interference. Furthermore, we show the metric to be robust within sub-optimal, lower complexity receiver architectures.

INTRODUCTION

The migration toward the integrated network enhanced telemetry (iNET) system introduces a new challenge of defining adaptive modulation and coding algorithms for the telemetry community. Adaptive modulation and coding schemes have been widely used in several Long Term Evolution (LTE) and Wi-Fi standards [1-2]. Similar adaptive algorithms have not yet been applied to aeronautical telemetry. In order to accomplish this task, the adaptive algorithm must employ two distinct modulation waveforms defined in iNET: 1) telemetry group SOQPSK (SOQPSK-TG) and 2) OFDM. Solving this task involves a multi-scheme adaptation, in which both SOQPSK and OFDM are used under the same decision rule. Georgia Tech Research Institute (GTRI) has investigated adaptive modulation and coding scheme for aeronautical telemetry, developed an algorithm that employs both modulation types, validated its performance via simulations, and shown operation in a laboratory environment. The performance of an adaptive scheme has shown to have 30% to 340% goodput performance improvement over a baseline scheme in various static telemetry channel models [1].

To further raise the technology readiness level (TRL) of using adaptive schemes in aeronautical telemetry, GTRI continued this effort by implementing the design onto a software defined radio (SDR) platform for test range demonstration. The transmitter hardware is composed of a National Instruments (NI) PXIe-7975R FlexRIO FPGA module, an NI 5791 RF transceiver module, an NI 8135 controller. The receiver hardware is composed of a Linux server with a Xilinx VC707

development card, a 4DSP FMC150 analog to digital converter card, and a custom built RF downconverter.

This paper focuses adaptation selection criteria implemented in the VC707 card. The field programmable gate array (FPGA) implementation is processing constrained and as such the efficiency of the adaptation rule must be mathematically simplified for the FPGA. The first part of the paper will discuss the hardware system and the adaptation algorithm developed in previous efforts. This will be followed by a description of a new link quality metric that exploits LDPC decoder information and an update on the system architecture requirement to enable this feature. The conclusion shows that utilizing the LDPC decoder iteration count can lead to a simpler adapter architecture that can be implemented in an FPGA.

BACKGROUND

In our previous work [2], we implemented a transceiver that employs both iNET waveforms: SOQPSK-TG and OFDM. In addition, LDPC [3] was used as the forward error correction (FEC) code. The top-level architecture of this system is shown in Figure 1. The objective of developing such a system is to demonstrate an adaptive algorithm that can adjust the waveform and FEC code based on an approximation of the link quality. One note of interest pertaining to Figure 1 is that Link Dependent Adaptive Radio's (LDAR) adapter is driven by the signal-to-noise ratio (SNR) estimator, which is approximated using EVM for OFDM and dispersion for SOQPSK.

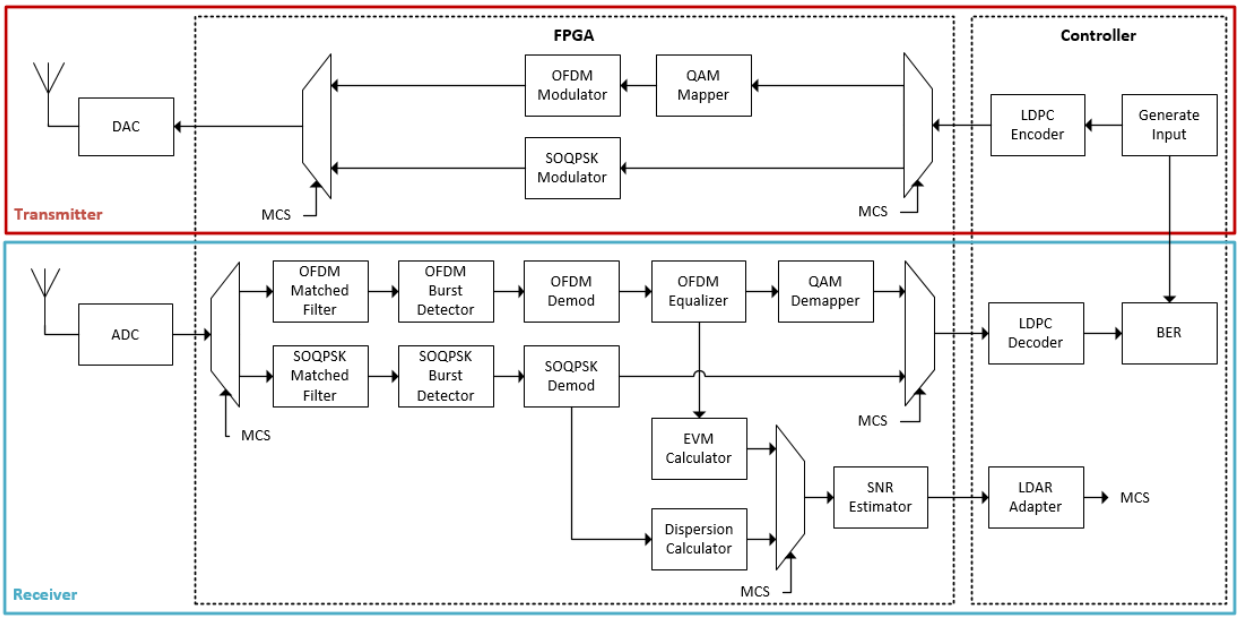

Figure 1. LDAR transceiver top-level system diagram.

In [2], we developed and demonstrated an adaptive algorithm for an added white Gaussian noise (AWGN) channel. This is done by using an approximation between dispersion and SNR. The problem arises when the channel is no longer AWGN. The dispersion equation for non-AWGN channel, derived in [4], is shown in (1)

$$Dispersion = 2\sum_{l=0}^{L-1}\sum_{m=0}^{M-1}|h_l|^2|h_m|^2 + \sum_{l=0}^{L-1}|h_l|^4 + 2\left[\left(\frac{EVM}{\frac{1}{N}\sum_{jj=1}^{N}\left|H_{jj}^{-1}\right|^2}\right)^2 + \frac{EVM}{\frac{1}{N}\sum_{jj=1}^{N}\left|H_{jj}^{-1}\right|^2}\right] - 1 \qquad (1)$$

As can be seen, the complexity of (1) is much greater than the assumptions made in [2]. GTRI investigated the assumptions made in [4] to understand if (1) could be used in a realistic channel. The investigation motivated the work presented in this paper.

LINK QUALITY METRIC

Previously, we had used an approximation of SNR to determine the adaptation algorithm. The waveform and FEC code would be adjusted depending on the approximated SNR. To expand this to a generic form, a link quality metric is defined. When we refer to the "link," we are speaking about the received signal strength versus all physical impairment (e.g. multipath propagation, interference, and noise) of the environment over which the communications take place. The "link" also encompasses the choice of modulation and coding as well as the transceiver implementation. From the perspective of the system designer, the link quality metric should take all of these elements into account: mode of operation, transceiver complexity, and the physical communications link.

The link metric can be seen as a measure of link quality from the viewpoint of the receiver. Ideally, it would incorporate all the physical channel impairments as well as any non-ideal implementations in other parts of the transceiver. If we focus specifically on the LDPC decoder for a quantization of the link quality metric, this would return a consistent number regardless of waveform or complexity of the system. Specifically, we are going to examine the number of iterations required for the LDPC to converge.

To design an adaptive algorithm that can be efficiently implemented onto an FPGA, GTRI investigated the potential of using LDPC decoder iteration count as a driver for adaptive modulation and coding algorithms. The LDPC decoder used here is a soft decision decoder developed by NASA's JPL [3], which makes use of the log-likelihood ratio (LLR) information that contains some intrinsic knowledge of the channel properties. The decoder, then, gains some extrinsic knowledge of the code constraints during one of its decoding iterations. This information is used as the a priori information for the subsequent decoding iterations until the valid codeword is found or the maximum number of iterations has passed. An in-depth explanation of a soft decision LDPC decoder can be found in Chapter 2 of [5].

Using the soft-decision decoder, the bit error rate (BER) and LDPC decoder iteration plots for all available LDAR modulation and coding schemes (MCS) for an AWGN channel is shown in Figure 2. In this figure, the black lines represent no LDPC code, and the blue, red, and magenta lines represent 4/5, 2/3, and 1/2 rates LDPC for all modulations, respectively. The maximum decoding iterations for all three LDPC code rates are set to 10, which means the decoder has a maximum of 10 tries to perform the syndrome check to determine if the codeword is valid. It can be clearly seen in Figure 2 that there is a direct correlation between the BER curves and the number of LDPC

iterations. As the SNR increases for a particular MCS, the BER and decoder iterations both decrease.

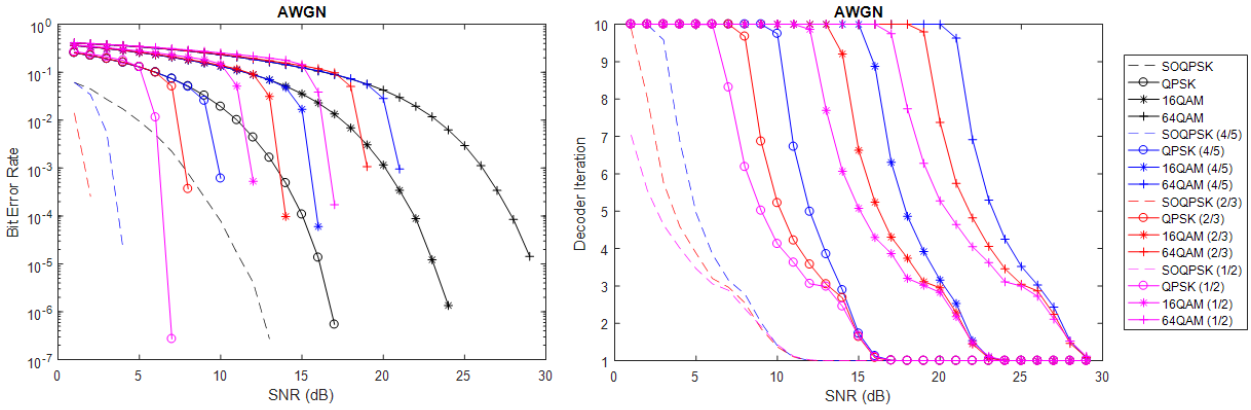

Figure 2. BER and decoder iteration counts for all LDAR MCS selections.

Another important note relating to Figure 2 is that at certain SNRs, the performance of all three code rates start to converge. Using SOQPSK (dash lines) as an example, at approximately 8 dB, the number of iterations for all three code rates slowly converge as the SNR increases. This behavior indicates that as the SNR increases the effects of the LDPC codes slowly diminishes and converges with the uncoded BER curves. This information gives the system designer an advantage of knowing when to switch to a MCS with higher data throughput or back-off to a more robust MCS to overcome channel impairments.

SYSTEM DESIGN

The BER and decoding iterations performance shown in Figure 2 highly correlates with how the communications system is designed. This section highlights some of the important blocks that are required to produce the results shown throughout this paper. One of the most important components is the LDPC encoder and decoder pair since the channel metric we are evaluating relies heavily on the number of LDPC decoding iterations. Another important component pertaining to the performance of the system is the equalizer. The following sub-sections highlight the equalizers used in both SOQPSK and OFDM demodulators.

A. SOQPSK

Due to the system requirement for soft decision inputs, a symbol-by-symbol (SxS) OQPSK detector is employed over a Viterbi detector. The soft decision of an SxS OQPSK detector is defined by the real and imaginary parts of the symbol when the sample number is even and odd, respectively [6]. The block diagram for SOQPSK simulation is shown in Figure 3, where the bits are encoded and modulated. The modulated signals are then filtered by one of the multipath channels shown in Figure 5. To overcome the inter-symbol interferences (ISI) resulting from the multipath propagation, an equalizer is used for the SOQPSK signal. Various equalization techniques for SOQPSK have been studied in [7]. The results have shown the performance

difference between a 4-state trellis detector and a symbol-by-symbol detector with equalizer is around 0 to 2 dB. The minimum mean-squared error (MMSE) equalizer used here is shown in (2),

$$c(n) = \boldsymbol{R}_{yy}^{-1} R_{xy} \tag{2}$$

where $\boldsymbol{R}_{yy}$ is a convolution matrix derived from the autocorrelation of the received preambles, and R_{xy} is the cross-correlation of the transmitted and received preambles. The derived equalizer coefficients, $c(n)$, are used to attempt to *undo* the effects of the multipath channel.

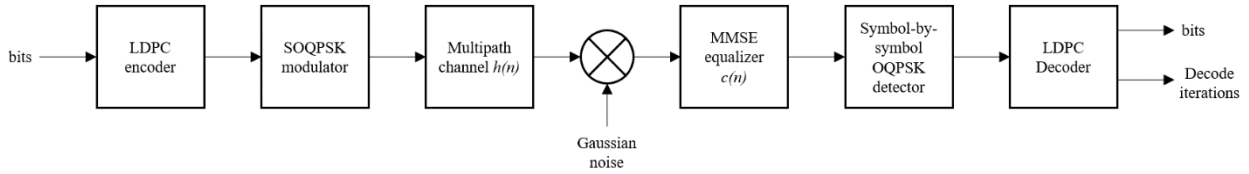

Figure 3. Block diagram for the simulation procedure.

B. OFDM

For OFDM, the block diagram is shown in Figure 4. The soft decisions are computed in the symbol demapper. The difference between SOQPSK and OFDM is that the receiver signal processing is mainly done in the frequency domain for OFDM. A major advantage of OFDM is its ability to easily adapt to frequency-selective channels without complex time-domain equalization. In the frequency domain, the equalizer becomes a one tap multiplication per data subcarrier, and allows for a simpler and more efficient receiver design. A more in-depth description for each of these blocks in Figure 4 can be found in [2].

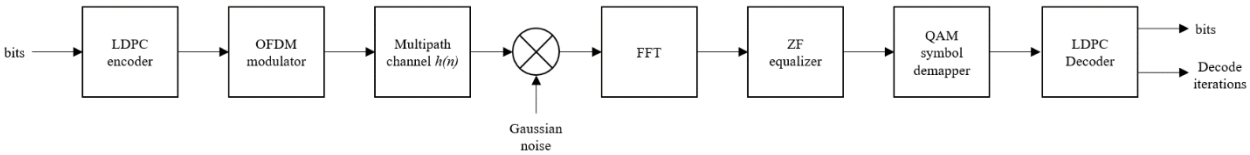

Figure 4. Block diagram for OFDM simulation.

PERFORMANCE RESULTS

To truly validate the usefulness of this technique, some multipath channels are used. The simulations were performed over 10 representative channels derived from one of the channel sounding measurements conducted at Edwards Air Force Base [8]. The corresponding frequency response plots are shown in Figure 5.

The simulated results for these channels are shown in Figures 6 and 7. In both figures, each subplot represents a mode of operation (or MCS), the y-axis of each subplot shows the channel number, and the x-axis shows the SNR in dB. The BER threshold plots of all LDAR modes of operation in all 10 channels are shown in Figure 6. In this figure, the MCS of each subplot is identified by its title, and the BER threshold is defined as 1×10^{-5}, meaning that the line is no longer displayed when the BER is greater than the defined threshold. If the BER is lower than the threshold for a given

SNR, the lines show a green square. The top row of the Figure 6 does not have any FEC code applied and the resulting BER threshold is reached sooner. The second row is 4/5 code rate, third row is 2/3 code rate, and fourth row is 1/2 code rate.

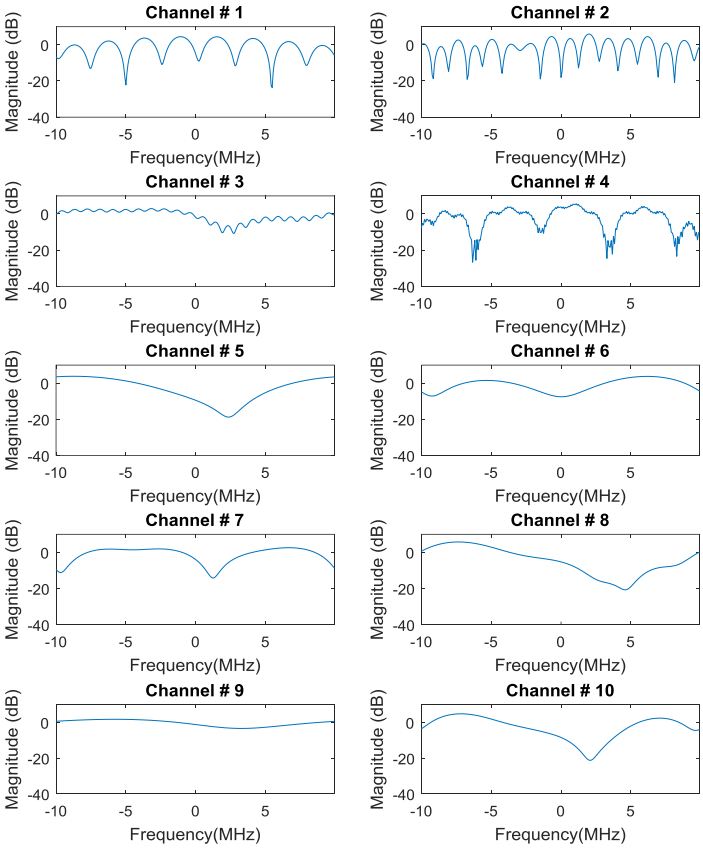

Figure 5. Frequency response plots of the representative channels at Edwards AFB.

In Figures 6, it can be seen that the system becomes more resilient to noise as the code rate decreases. This shows a relation between the link quality metric and the SNR/BER for these channels. The previous LDAR system utilizes SNR approximations to determine the adaptation selection. However, as can be seen in Figure 6, there is a high degree of uncertainty based upon the channel of operation. Switching the MCS based off of an SNR approximation alone would not be enough to take into account the BER caused by the individual channels. For instance, channel 6 can be seen to have a higher bit error rate for the same SNR value as compared to channel 9 for all MCS selections. The previous LDAR system attempted to predict the most robust MCS based on an assumption as to the channel of operation. Using a single, unified link quality metric can account for all of these uncertainties, the LDAR adaptive algorithm can be simplified. Based on the current definition of "link," the adapter would view the mode of operation, the channel properties, as well as the equalizer effects as part of the link quality metric.

The number of LDPC decoder iterations for each MCS is shown in Figure 7. The maximum number of decoding iterations is set to 10. In this figure, the color scale on the right reflects the number of iterations for convergence. In the case where the decoder does not converge, the color is shown in white. When Figures 6 and 7 are compared, it can be seen that there is a direct

correlation between the convergence rate and the BER for all modes of operations in all ten channels. Utilizing the LDPC decoder iteration count, a link quality metric can be obtained. This metric captures a complete characterization of the transceiver complexity, channel, and the transmission mode. This allows for even more accurate control of the adaptability than the approximation of SNR since it includes an added layer of link quality information.

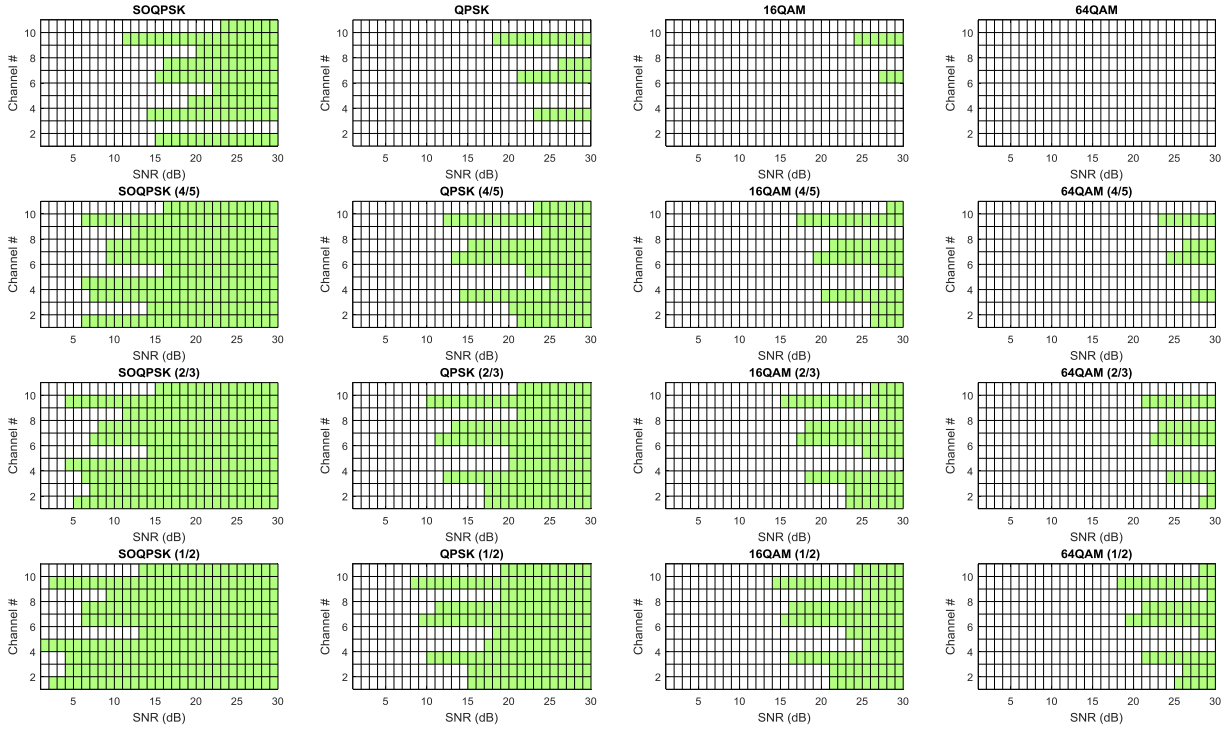

Figure 6: LDAR MCS BER thresholds in all ten Edwards AFB channels.

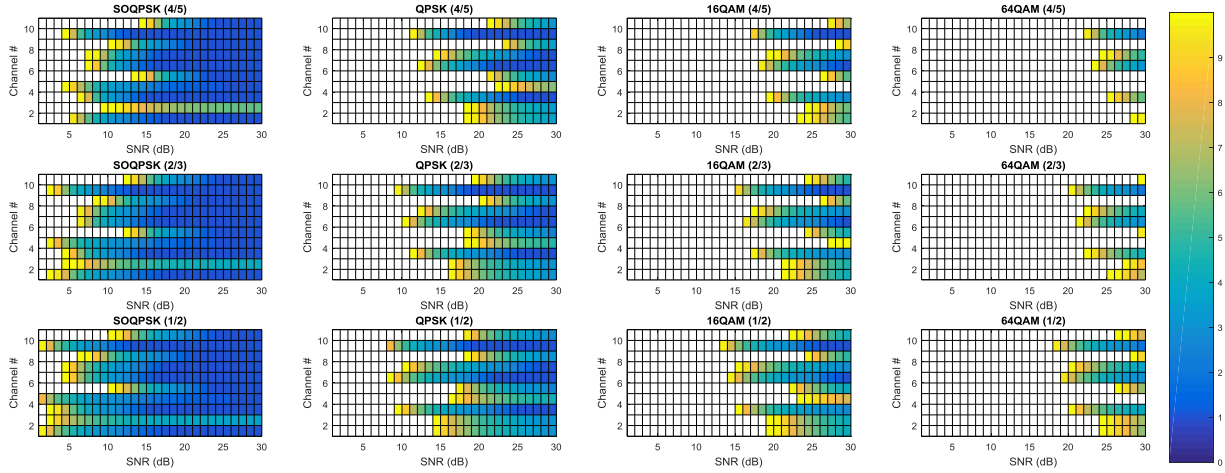

Figure 7: LDPC iteration counts for all LDAR MCS in all ten Edwards AFB channels.

Figure 8 illustrates the top-level block diagram utilizing the LDPC decoder iteration count to adapt the transmission mode of operations. This not only reduces computational complexity but also provides a more accurate characterization over the link quality.

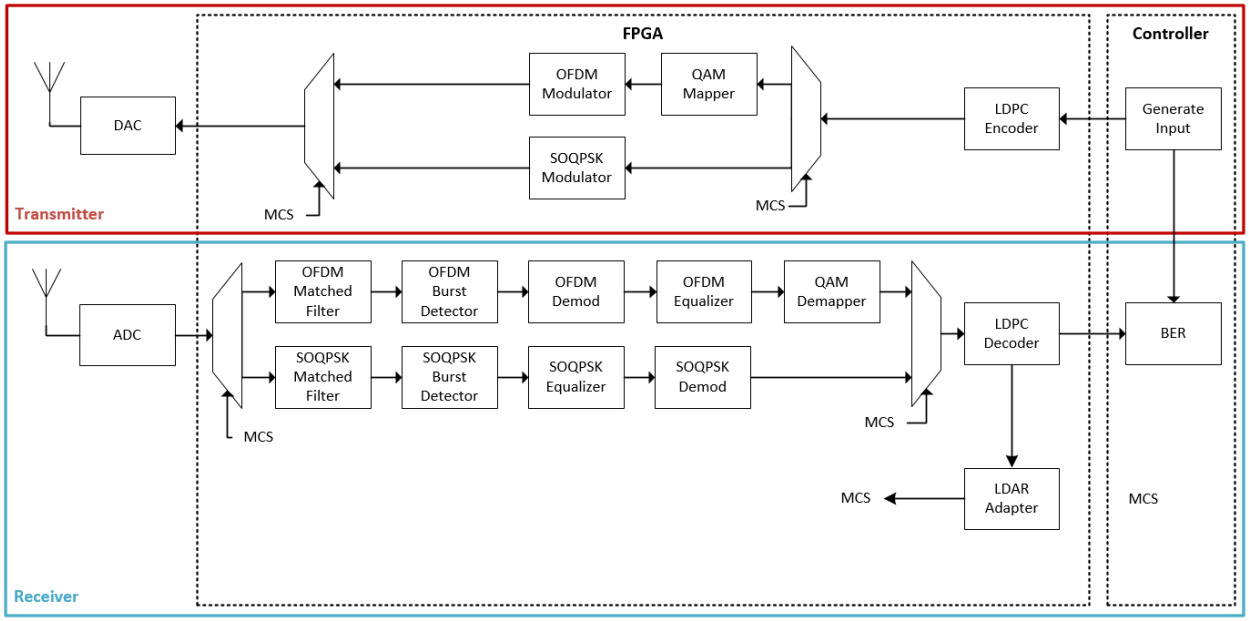

Figure 8: Top-level architecture for next generation LDAR transceiver.

The adaptation scheme now simplifies to incrementing or decrementing the MCS based on a low and a high threshold applied to the LDPC iteration count. These thresholds could be adjusted based on the acceptable BER for the given test. Given the case of a rapidly deteriorating channel (such as an aircraft executing a fast maneuver), the number of decoding iterations for a particular modulation would suddenly increase over a short amount of time, prompting the adapter to "back-off" and jump to an MCS that is more robust. Conversely, if the LDPC iteration counts decrease more slowly over time, a more spectrally efficient waveform such as OFDM can be selected. Table 1 shows the possible combinations of modulations and code rates along with the MCS selection and the throughput. Please note that the current LDAR transceiver have not implemented all of the LDPC codes and the MMSE equalizer for SOQPSK-TG.

Table 1: Adaptation Selection

MCS	Modulation	Code Rate	Throughput (Mbps)
1	SOQPSK	1/2	3.75
2	SOQPSK	2/3	5
3	SOQPSK	4/5	7.5
4	QPSK (OFDM)	1/2	9.6
5	QPSK (OFDM)	2/3	12.8
6	QPSK (OFDM)	4/5	15.36
7	16 QAM (OFDM)	1/2	19.2
8	16 QAM (OFDM)	2/3	25.6
9	64 QAM (OFDM)	1/2	28.8
10	16 QAM (OFDM)	4/5	30.72
11	64 QAM (OFDM)	2/3	38.4
12	64 QAM (OFDM)	4/5	46.08

CONCLUSION AND FUTURE WORK

This paper has defined a link quality metric for adaptability that includes the transceiver design complexity and the channel properties. We have shown that the LDPC iteration count is a valid metric to utilize for the link quality estimation. Finally, a transceiver architecture with a simplified adapter has been realized in hardware to exploit the LDPC decoder iteration count to adjust the modulation and coding scheme (MCS) selection based on the link quality.

The future work includes completing system integration, hardware in the loop tests, and a field test of the LDAR system.

ACKNOWLEDGEMENT

This project is funded by the Test Resource Management Center (TRMC) Test and Evaluation/Science & Technology (T&E/S&T) Program through the U.S. Army Program Executive Office for Simulation, Training and Instrumentation (PEO STRI) under Contract No. W900KK-13-C-024. The public release number is 412TW-PA-17322.

REFERENCES

[1] E. Wang, B. T. Walkenhorst and J. Han, "A Simulation Testbed for Adaptive Modulation and Coding in Airborne Telemetry," in *Proceedings of the International Telemetering Conference*, San Diego, CA, Oct. 2014.

[2] E. Wang and T. Brothers, "OFDM and SOQPSK transceiver hardware implementation with preliminary results," in *Proceedings of the International Telemetering Conference*, Glendale, AZ, 2016.

[3] Consultive Committee for Space Data System (CCSDS), "Low density parity check codes for use in near-Earth and deep space applications (131.1-O-2 Orange Book)," Sep. 2007.

[4] J. Han, B. Walkenhorst and E. Wang, "Adaptive modulation schemes for OFDM and SOQPSK using error vector magnitude (EVM) and Godard dispersion," in *Proceedings of the International Telemetering Conference*, San Diego, CA, October 2014.

[5] S. Johnson, Iterative error correction: turbo, low-density parity-check and repeat-accumulate, Cambridge University Press, 2010.

[6] E. Perrins, "FEC systems for aeronautical telemetry," *IEEE Trans on Aerospace and Electronic Systems*, vol. 49, no. 4, pp. 2340-2352, 2013.

[7] M. Rice, M. S. Afran, M. Saquib, A. Cole-Rhodes and F. Moazzami, "A comparison of three equalization techniques for iNET-formatted SOQPSK-TG," in *Proceedings of the International Telemetering Conference*, San Diego, CA, October 2014.

[8] M. Rice and M. Jensen, "A comparison of L-band and C-band multipath propagation at Edwards AFB," in *Proceedings of the International Telemetering Conference*, Las Vegas, NV, October 2011.

[9] integrated Network Enhanced Telemetry (iNET), "Radio Access Network (RAN) Standard," 2013.

[10] E. Hosseini and E. Perrins, "Timing, Carrier, and Frame Synchronization of Burst-Mode CPM," *IEEE Transactions on Communications*, vol. 61, no. 12, pp. 5125-5138, 2013.

[11] J. Chen, A. Dholakia, E. Eleftheriou, M. Fossorier and X.-Y. Hu, "Reduced-complexity decoding of LDPC codes," *IEEE Transaction on Communications*, vol. 53, no. 7, pp. 1288-1299, 2005.

[12] D. N. Godard, "Self-recovering equalization and carrier tracking in two-dimensional data communication systems," *IEEE Trans. Acoust., Speech, Signal Process.*, vol. 31, no. 2, pp. 459-472, Apr. 1983.

[13] 3GPP TS 36.521-1 V9.3.0, "User equipment (UE) conformance specification, radio transmission and reception, part 1: conformance testing".

[14] IEEE 802.11 working group, "IEEE P802.11n/D0.02," Feb 2006.